



Universiteit  
Leiden  
The Netherlands

## **Progressive white matter injury in preclinical Dutch cerebral amyloid angiopathy**

Shirzadi, Z.; Yau, W.Y.W.; Schultz, S.A.; Schultz, A.P.; Scott, M.R.; Goubran, M.; ... ; DIAN Investigators

### **Citation**

Shirzadi, Z., Yau, W. Y. W., Schultz, S. A., Schultz, A. P., Scott, M. R., Goubran, M., ... Chhatwal, J. P. (2022). Progressive white matter injury in preclinical Dutch cerebral amyloid angiopathy. *Annals Of Neurology*, 92(3), 358-363. doi:10.1002/ana.26429

Version: Publisher's Version

License: [Creative Commons CC BY 4.0 license](https://creativecommons.org/licenses/by/4.0/)

Downloaded from: <https://hdl.handle.net/1887/3502273>

**Note:** To cite this publication please use the final published version (if applicable).

# Progressive White Matter Injury in Preclinical Dutch Cerebral Amyloid Angiopathy

Zahra Shirzadi, PhD<sup>1</sup>,  
 Wai-Ying W. Yau, MD<sup>1</sup>,  
 Stephanie A. Schultz, PhD,<sup>1</sup>  
 Aaron P. Schultz, PhD,<sup>1</sup>  
 Matthew R. Scott, BSc,<sup>1</sup>  
 Maged Goubran, PhD,<sup>2</sup>  
 Parisa Mojiri-Forooshani, MSc,<sup>2</sup>  
 Nelly Joseph-Mathurin, PhD<sup>1,3</sup>,  
 Kejal Kantarci, MD<sup>4</sup>,  
 Greg Preboske, MSc,<sup>4</sup>  
 Marieke J. H. Wermer, MD, PhD,<sup>5</sup>  
 Clifford Jack, MD,<sup>4</sup>  
 Tammie Benzinger, MD, PhD,<sup>3</sup>  
 Kevin Taddei, BSc,<sup>6</sup>  
 Hamid R. Sohrabi, PhD,<sup>7</sup>  
 Reisa A. Sperling, MD,<sup>1</sup>  
 Keith A. Johnson, MD,<sup>1</sup>  
 Randall J. Bateman, MD,<sup>3</sup>  
 Ralph N. Martins, PhD,<sup>6</sup>  
 Steven M. Greenberg, MD, PhD,<sup>1</sup> and  
 Jasmeer P. Chhatwal, MD, PhD,<sup>1</sup>  
 DIAN Investigators

Autosomal-dominant, Dutch-type cerebral amyloid angiopathy (D-CAA) offers a unique opportunity to develop biomarkers for pre-symptomatic cerebral amyloid angiopathy (CAA). We hypothesized that neuroimaging measures of white matter injury would be present and progressive in D-CAA prior to hemorrhagic lesions or symptomatic hemorrhage. In a longitudinal cohort of D-CAA carriers and non-carriers, we observed divergence of white matter injury measures between D-CAA carriers and non-carriers prior to the appearance of cerebral microbleeds and >14 years before the average age of first symptomatic hemorrhage. These results indicate that white matter disruption measures may be valuable cross-sectional and longitudinal biomarkers of D-CAA progression.

ANN NEUROL 2022;92:358–363

Cerebral amyloid angiopathy (CAA) is a form of cerebral small vessel disease that is a common cause of intracerebral hemorrhage and a contributor to cognitive

impairment.<sup>1–3</sup> CAA commonly co-occurs with parenchymal  $\beta$ -amyloid deposition (as in Alzheimer's disease) but can also occur independently.<sup>4</sup> Although most cases of CAA are sporadic, several genetic variants in amyloid precursor protein (APP) have been shown to lead to autosomal dominant forms of CAA. The most common type is Dutch-type CAA (D-CAA), which is caused by a point mutation in APP (E693Q<sup>5</sup>). D-CAA becomes symptomatic at a younger age compared to the sporadic form, yet presents with similar clinical and radiological manifestations as sporadic CAA.<sup>6</sup> By virtue of its early age of onset and complete penetrance, the study of D-CAA provides a unique window into pre-symptomatic CAA pathophysiology. D-CAA is a lethal, orphan disease for which there are few focused clinical trials. This is partly due to the difficulty in identifying suitable biomarkers of disease progression in early stages, prior to the emergence of cerebral hemorrhage. Building on prior cross-sectional work suggesting white matter disruption may occur prior to symptomatic hemorrhage in D-CAA,<sup>7</sup> we examined the progression of white matter changes in a longitudinal cohort of individuals with D-CAA. To investigate white matter changes, we used white matter hyperintensity (WMH) volume and peak width of skeletonized mean diffusivity (PSMD) – a recently developed diffusion-based measure that is sensitive to cerebrovascular injury.

## Methods

### Participants

Neuroimaging data from 20 participants (9 D-CAA carriers and 11 non-carriers from the same families) in the Dominantly Inherited Alzheimer Network (DIAN; NIA-U19-AG032438) were used in this study. Full procedures for DIAN are described elsewhere.<sup>8,9</sup> One participant in

From the <sup>1</sup>Department of Neurology, Massachusetts General Hospital, Harvard Medical School, Boston, MA; <sup>2</sup>Physical Sciences Platform and Hurvitz Brain Sciences Program, Sunnybrook Research Institute, University of Toronto, Toronto, Ontario, Canada; <sup>3</sup>Mallinckrodt Institute of Radiology, Washington University School of Medicine, Saint Louis, MO; <sup>4</sup>Department of Radiology, Mayo Clinic, Rochester, MN; <sup>5</sup>Department of Neurology, Leiden University Medical Centre, Leiden, The Netherlands; <sup>6</sup>Centre of Excellence for Alzheimer's Disease Research and Care, School of Medical and Health Sciences, Edith Cowan University, Joondalup, Western Australia, Australia; and <sup>7</sup>Centre for Healthy Ageing, Health Future Institute, Murdoch University, Murdoch, Western Australia, Australia

Address correspondence to Prof Chhatwal, Department of Neurology, Massachusetts General Hospital, Harvard Medical School, 55 Fruit Street, Boston, MA 02114, USA. E-mail: [chhatwal.jasmeer@mgh.harvard.edu](mailto:chhatwal.jasmeer@mgh.harvard.edu)

Received Jan 6, 2022, and in revised form Jun 3, 2022. Accepted for publication Jun 4, 2022.

View this article online at [wileyonlinelibrary.com](http://wileyonlinelibrary.com). DOI: 10.1002/ana.26429.

the non-carrier group had a Clinical Dementia Rating (CDR) of 0.5. One D-CAA carrier had a CDR of 0 at baseline, but was CDR 0.5 at follow-up. All other participants were CDR = 0 throughout the study. All study procedures received approval from participating institutions. Participants gave informed consent prior to the performance of any study procedures.

### Image Acquisition and Processing

The following magnetic resonance (MR) images (3 T) were used: (1) T1-weighted (T1w) MPRAGE: TR/TE/TI = 2,300/2.95/900 ms, dimensions =  $1.1 \times 1.1 \times 1.2 \text{ mm}^3$ ; (2) 2D axial fluid-attenuated inversion recovery (FLAIR): TR/TE/TI = 9,000/91/2,500 ms, dimensions =  $0.86 \times 0.86 \times 5 \text{ mm}^3$ ; (3) 2D EPI diffusion tensor imaging (DTI): TR/TE = 8,100/87 ms, dimensions =  $2.5 \times 2.5 \times 2.5 \text{ mm}^3$ , number of directions = 64,  $b$ -value = 1,000 s/mm<sup>2</sup>; (4) susceptibility weighted image: TR/TE = 28/20 ms, dimensions =  $0.7 \times 0.7 \times 2.4 \text{ mm}^3$  (baseline visits for all participants) or T2\*-weighted gradient echo weighted image: TR/TE = 650/20 ms, dimensions =  $0.8 \times 0.8 \times 4 \text{ mm}^3$ .

We segmented WMH on FLAIR images using the HyperMapp3r algorithm (<https://hypermapp3r.readthedocs.io/>). HyperMapp3r is a convolutional neural network-based segmentation algorithm that uses T1w, FLAIR, and brain mask images to generate WMH predictions in the T1w subject space. This pipeline outperforms other automated WMH segmentation procedures in quantifying deep and small WMH.<sup>10</sup> For illustrations of white matter lesions, WMH masks were co-registered to MNI standard space using the FLIRT tool (<https://fsl.fmrib.ox.ac.uk/fsl/flwiki/FLIRT>) in FSL6.0.1. Subsequently, a WMH probability map was created for baseline data of carriers to visualize the spatial pattern of lesions. Last, we calculated lobar WMH volumes using the MNI structural atlas.

We estimated PSMD from DTI using a publicly available script (<http://www.psmddmarker.com>).<sup>11</sup> This pipeline preprocessed diffusion magnetic resonance imaging (MRI; eddy current and motion correction) followed by tensor fitting, skeletonization of the data, and histogram analysis using FSL6.0.1 tools, including Tract-Based Spatial Statistics procedure (<http://fsl.fmrib.ox.ac.uk/fsl/flwiki/TBSS>) and fractional anisotropy template (<https://fsl.fmrib.ox.ac.uk/fsl/flwiki/Atlases,fsl>).

Susceptibility weighted/T2\*-weighted gradient echo images were visually inspected for the presence of sulcal blood and macro/microbleeds by radiologists at the Mayo Clinic in Rochester.<sup>12,13</sup> Small lesions ( $\leq 10 \text{ mm}$ ) that were dissociable from small vessels were counted as definite microbleeds.

### Statistical Analyses

Statistical analyses were performed in R (version 4.0.2) and nominal  $p$  values are reported. Independent  $t$  test, Wilcoxon rank test, and chi-squared tests were used to compare D-CAA carrier and non-carrier demographics and clinical measures. Pearson correlations were used to investigate the association between the WMH volume (log-transformed to reduce skewness) and PSMD. Linear mixed-effect models assessed the longitudinal effects of D-CAA carriage and interactions with age for each marker. As in prior DIAN studies, we estimated the age of divergence between D-CAA carriers and non-carriers for WMH and PSMD using Hamiltonian Markov chain

**TABLE. Participants' Demographics and Study Information**

	D-CAA carrier (n = 9)	D-CAA non-carrier (n = 11)
Age at baseline, years	44.9 $\pm$ 6.0	40.2 $\pm$ 8.3
Sex, female/male	6/3	7/4
APOE $\epsilon 4$ , -/+	8/1	8/3
Education, years	14 $\pm$ 2.5	14 $\pm$ 3.0
MMSE at baseline	28.3 $\pm$ 1.4	28.5 $\pm$ 1.9
MMSE at last visit	28.6 $\pm$ 1.1	28.4 $\pm$ 1.6
CDR-SOB at baseline, 0/0.5	9/0	10/1
CDR-SOB at last visit, 0/0.5	8/1	10/1
Follow-up time, years	3.7 $\pm$ 2.1	3.0 $\pm$ 2.3
Hypercholesterolemia, yes/no	0/9	0/11
Hypertension, yes/no	1/8	3/8
Diabetes, yes/no	0/9	0/11
Obesity, body mass index $>35$ , yes/no	0/9	0/11
WMH volume at baseline, mm <sup>3</sup>	6,917 $\pm$ 9,218	350 $\pm$ 419
PSMD at baseline, $\times 10^{-4} \text{ mm}^2/\text{s}$	2.93 $\pm$ 0.6	2.26 $\pm$ 0.2

Mean  $\pm$  standard deviation or numbers are reported. There are no significant differences between the carriers and non-carriers ( $p > 0.1$ ). APOE  $\epsilon 4$  (-/+) = apolipoprotein E allele  $\epsilon 4$  status negative/positive; CDR-SOB = clinical dementia rating sum of the boxes; MMSE = mini-mental state examination; PSMD = peak width of skeletonized mean diffusivity; WMH = white matter hyperintensity.

Monte Carlo analyses (<http://mc-stan.org/>). Subsequently, the distribution of parameter estimates across iterations was assessed to generate 95% credible intervals of the model fit. The age of divergence was determined as the point where 95% credible intervals of the difference distribution did not overlap 0.<sup>14</sup>

Last, we performed a series of sensitivity analyses to (1) investigate regional specificity of WMH in differentiating carriers and non-carriers; (2) restrict analysis to only D-CAA carriers without any radiological evidence of macro/microbleeds; and (3) restrict analysis to only participants with a global CDR of zero.

## Results

D-CAA carriers and non-carriers had similar demographics (see the Table). The mutation carriers demonstrated periventricular WMH in posterior cortical regions, whereas no deep WMHs were observed (Fig 1A). Similarly, higher levels of mean diffusivity were observed in the posterior regions (Fig 1B). White matter measures were significantly different between carriers and non-carriers at baseline (see the Table,  $p < 0.005$ ). PSMD and WMH were strongly intercorrelated ( $r = 0.8$ ,  $p < 0.001$ ).

Rates of white matter change were assessed in participants with available longitudinal MRI ( $n = 16$ , 8 carriers,

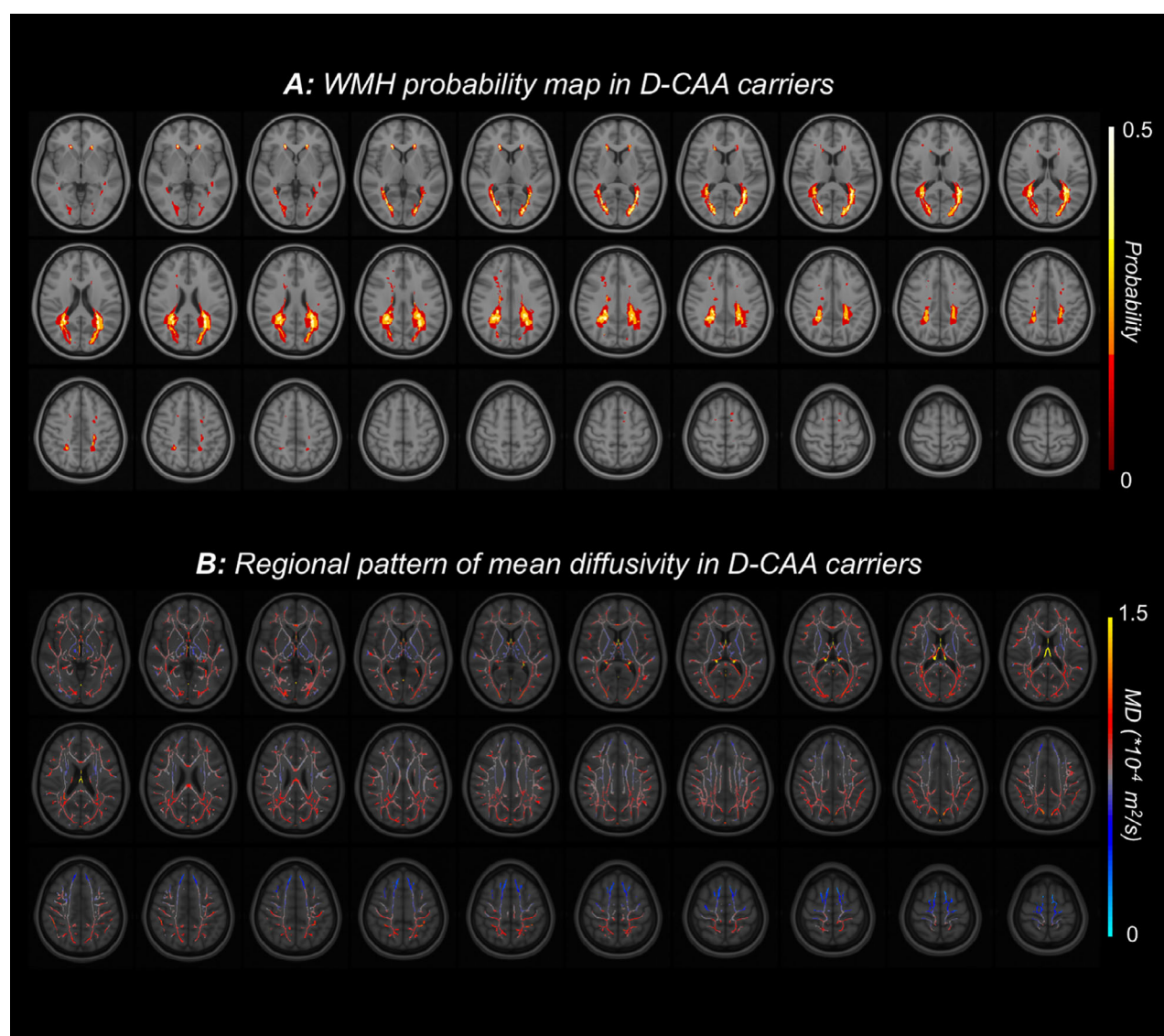


**FIGURE 1:** Spatial patterns of white matter injury in D-CAA. (A) FLAIR-based white matter hyperintensity (WMH) probability map in D-CAA carriers showing a posterior predominance. Individual images were placed in MNI space, and voxels are colored by the probability of a white matter lesion being present in this cohort. (B) Diffusion based mean diffusivity in the white matter skeleton. Individual mean diffusivity images were placed in MNI space, and voxels are colored by the average value across D-CAA carriers in this cohort. D-CAA = Dutch-type cerebral amyloid angiopathy; FLAIR = fluid-attenuated inversion recovery.

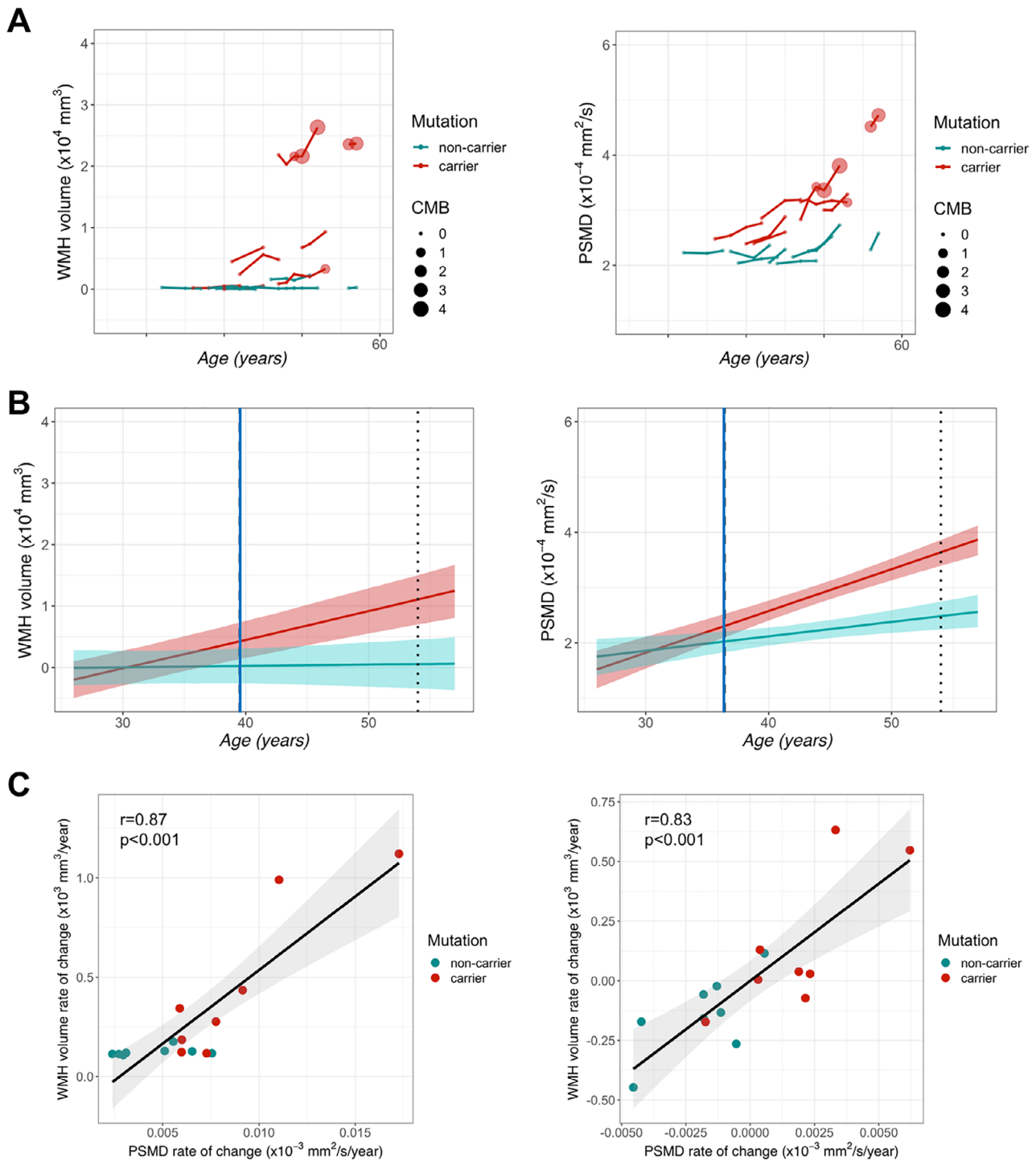


**FIGURE 2:** Longitudinal white matter measures. (A) Measures of white matter injury in D-CAA mutation carriers and non-carriers are plotted over time, using age as a temporal reference. Lines shown connect measurements from an individual participant during longitudinal follow-up. Please note that exact ages are not shown to maintain blinding of D-CAA carrier status. The size of circles represents the number of definite cerebral microbleed (CMB) in each visit. (B) Illustration of divergence analyses for D-CAA carriers (red) and non-carriers (teal). The standardized rate of change for each white matter measure based on model fit is depicted in each line. The blue solid line shows the age of divergence for each measure between D-CAA carriers and non-carriers while the dotted line indicates the average age of the first hemorrhage in D-CAA. The shaded area shows the 95% credible intervals for each model fit. (C) The relationship between WMH and PSMD rate of change without (left) and with (right) adjustment for age. D-CAA = Dutch-type cerebral amyloid angiopathy; PSMD = peak width of skeletonized mean diffusivity; WMH = white matter hyperintensity.

8 non-carriers, and 52 annual visits). White matter injury measures increased over time, particularly in older D-CAA carriers (Fig 2A). At a group level, rates of change in WMH and PSMD diverged between carriers and non-carriers at approximately age 40 years (Fig 2B), greater than 14 years prior to the average age of first symptomatic hemorrhage in D-CAA<sup>15</sup> and >10 years prior to the age of first microbleed in this cohort (Fig 2A). The predicted annual rate of change for carriers was 495 (95% confidence interval [CI] = 258–756) mm<sup>3</sup>/yr for WMH ( $t = 3.4$ ,  $df = 14.3$ ,  $p = 0.004$ ) and  $5.2 \times 10^{-6}$  (95% CI =  $1.9 \times 10^{-6}$ – $8.7 \times 10^{-6}$ ) mm<sup>2</sup>/s/yr for PSMD ( $t = 2.5$ ,  $df = 11.8$ ,  $p = 0.02$ ). The rates of change for WMH and PSMD were highly correlated (Fig 2C).

In the sensitivity analysis, we observed no significant effect of D-CAA carriage in frontal and temporal lobes; in contrast, effects of carrier state were observed for WMH in occipital ( $t = 2.5$ ,  $p = 0.02$ ) and parietal ( $t = 2.6$ ,  $p = 0.02$ ) lobes.

Only one D-CAA carrier had radiological evidence of microbleed and sulcal blood at baseline; 2 other participants developed microbleeds at follow-up visits (Fig 2A). Excluding these visits ( $n = 15$ , number of observations = 46) led to similar results with respect to rates of change in D-CAA carriers versus non-carriers: WMH ( $t = 2.8$ ,  $df = 5.1$ ,  $p = 0.03$ ) and PSMD ( $t = 3.1$ ,  $df = 33$ ,  $p = 0.004$ ). Similarly, excluding visits at which participants had CDR = 0.5 did not eliminate the observed effects (WMH:  $t = 3.2$ ,  $df = 14.6$ ,  $p = 0.006$ ; PSMD:  $t = 4.4$ ,  $df = 40$ ,  $p < 0.001$ ).

## Discussion

In this study, we observed clear signs of progressive white matter disruption visible on MRI in pre-symptomatic phases of D-CAA. This suggests that white matter injury in D-CAA precedes intracerebral hemorrhage, cerebral microbleeds, and cognitive decline – cardinal CAA-associated events. The findings also suggest that white matter changes may be usable as a biomarker in pre-symptomatic D-CAA, a stage of disease that is relatively lacking in biomarker measures that can be used in disease-modifying clinical trials. Patterns were similar across both FLAIR-based WMH and DTI-based PSMD. The longitudinal analyses recapitulated patterns seen in the cross-sectional data<sup>7</sup> and demonstrated that rates of change in white matter measures diverged between D-CAA carriers and non-carriers more than a decade prior to symptomatic hemorrhage in D-CAA.

Despite similar trajectories, the white matter measures examined in this study represent potentially distinct forms of white matter injury. The posterior predominance for WMH and lack of deep lesions is in line with the

recent finding in D-CAA that showed first cerebral hemorrhage in D-CAA is also more frequent in occipital lobe.<sup>16</sup> Moreover, prior reports demonstrated that blood vessel amyloid deposition in CAA may preferentially affect posterior brain regions,<sup>17</sup> and that posterior WMH are more closely related to elevated amyloid burden versus higher cardiovascular risk in older adults.<sup>18</sup> In comparison, PSMD is thought to represent axonal and myelin loss,<sup>19</sup> and possible structural disconnection between brain regions. Compared to other DTI measures, PSMD may offer greater power in quantifying white matter changes that result from cerebral small vessel disease.<sup>11</sup> Importantly, these measures were obtained from fully automated and accessible processing pipelines thus can be easily implemented in clinical trial settings.

Although both measures showed strong cross-sectional and longitudinal effects, we found WMH had a slightly larger effect in differentiating D-CAA carriers and non-carriers. The strength with which WMH differentiated D-CAA carriers and non-carriers may have been enhanced by the low levels of WMH in the relatively young non-carrier population, providing a strong contrast. The findings here regarding early changes in white matter are consistent with neuropathological examinations of end-stage D-CAA.<sup>20</sup> These prior neuropathological findings together with the imaging findings here strongly suggest white matter changes are prominent in early and late phases of D-CAA and, further, that CAA physiology should potentially be considered in the differential diagnosis of white matter disease more broadly.

Notably, the sample size in this study is relatively small, as D-CAA is a rare condition. Despite the small sample size, the observed effects were robust and consistent across white matter measures, suggesting that markers of white matter change used here can potentially be used as biomarker measures in clinical trials with a small number of participants.

Together, these results suggest that white matter injury occurs early in the D-CAA disease course and may provide powerful biomarkers for D-CAA clinical trials and research. Importantly, as the study of D-CAA can provide valuable insights into sporadic CAA, our findings strongly support assessing similar white matter changes in sporadic CAA.

## Acknowledgments

This work was supported by the National Institute of Neurologic Diseases and Stroke (R01NS070834) and the National Institute on Aging (Dominantly Inherited Alzheimer's Network; UF1AG032438; K23AG049087; P01AG036694). Zahra Shirzadi gratefully acknowledges a fellowship award from the Alzheimer's Society of Canada that supported this work. Last, data collection for this study was supported by the

National Health and Medical Research Council grant (APP1129627) to Ralph N. Martins.

This research was carried out in part at the Athinoula A. Martinos Center for Biomedical Imaging at the Massachusetts General Hospital, using resources provided by the Center for Functional Neuroimaging Technologies, *P41EB015896*, a P41 Biotechnology Resource Grant supported by the National Institute of Biomedical Imaging and Bioengineering (NIBIB), National Institutes of Health (NIH). This work also involved the use of instrumentation supported by the NIH Shared Instrumentation Grant Program and/or High-End Instrumentation Grant Program; specifically, grant numbers S10RR021110, S10RR023401, and S10RR023043.

## Author Contributions

Z.S., R.A.S., K.A.J., S.M.G., and J.P.C. contributed to the conception and design of the study. Z.S., W.W.Y., S.A.C., M.R.S., M.G., P.M.F., N.J.M., M.W., K.K., G.P., J.P.C., C.J., T.B., K.T., H.R.S., R.J.B., and R.N.M. contributed to the acquisition and analysis of data. Z.S., A.P.S., and J.P.C. contributed to drafting the text or preparing the figures.

## Potential Conflicts of Interest

There are no conflicts of interest relevant to the content of this study.

## References

- Charidimou A, Gang Q, Werring DJ. Sporadic cerebral amyloid angiopathy revisited: recent insights into pathophysiology and clinical spectrum. *J Neurol Neurosurg Psychiatry* 2012;83:124–137.
- Kazim SF, Ogulnick JV, Robinson MB, et al. Cognitive impairment after intracerebral hemorrhage: a systematic review and meta-analysis. *World Neurosurg* 2021;148:141–162.
- Boyle PA, Yu L, Nag S, et al. Cerebral amyloid angiopathy and cognitive outcomes in community-based older persons. *Neurology* 2015;85:1930–1936.
- Greenberg SM, Bacskai BJ, Hernandez-Guillamon M, et al. Cerebral amyloid angiopathy and Alzheimer disease — one peptide, two pathways. *Nat Rev Neurol* 2020;16:30–42.
- Levy E, Carman MD, Fernandez-Madrid LJ, et al. Mutation of the Alzheimer's disease amyloid gene in hereditary cerebral hemorrhage, Dutch type. *Science* 1990;248:1124–1126.
- van Rooden S, van der Grond J, van den Boom R, et al. Descriptive analysis of the Boston criteria applied to a Dutch-type cerebral amyloid angiopathy population. *Stroke* 2009;40(9):3022–7.
- Van Rooden S, Van Opstal AM, Labadie G, et al. Early magnetic resonance imaging and cognitive markers of hereditary cerebral amyloid angiopathy. *Stroke* 2016;47:3041–3044.
- Morris JC, Aisen PS, Bateman RJ, et al. Developing an international network for Alzheimer's research: the dominantly inherited Alzheimer network. *Clin Invest* 2012;2:975–984.
- Bateman RJ, Xiong C, Benzinger TLS, et al. Clinical and biomarker changes in dominantly inherited Alzheimer's disease. *N Engl J Med* 2012;367:795–804.
- Forooshani PM, Biparva M, Ntiri EE, et al. Deep Bayesian networks for uncertainty estimation and adversarial resistance of white matter hyperintensity segmentation. *bioRxiv* 2021;2021.08.18.456666. Available at: <http://biorxiv.org/content/early/2021/08/23/2021.08.18.456666.abstract>
- Baykara E, Gesierich B, Adam R, et al. A novel imaging marker for small vessel disease based on skeletonization of white matter tracts and diffusion histograms. *Annals of Neurology* 2016;80:581–592.
- Joseph-Mathurin N, Wang G, Kantarci K, et al. Longitudinal accumulation of cerebral microhemorrhages in dominantly inherited Alzheimer disease. *Neurology* 2021;96:e1632–e1645.
- Kantarci K, Gunter J, Tosakulwong N, et al. Focal hemosiderin deposits and beta-amyloid load in the ADNI cohort. *Alzheimers Dement* 2013;9(5 Suppl):S116–23.
- Preische O, Schultz SA, Apel A, et al. Serum neurofilament dynamics predicts neurodegeneration and clinical progression in presymptomatic Alzheimer's disease. *Nat Med* 2019;25:277–283.
- van Etten ES, Gurol ME, van der Grond J, et al. Recurrent hemorrhage risk and mortality in hereditary and sporadic cerebral amyloid angiopathy. *Neurology* 2016;87:1482–1487.
- Voigt S, Amlal S, Koemans EA, et al. Spatial and temporal intracerebral hemorrhage patterns in Dutch-type hereditary cerebral amyloid angiopathy. *Int J Stroke* 2021;174749302110570. doi:10.1177/17474930211057022. [Online ahead of print].
- Thal DR, Ghebremedhin E, Orantes M, Wiestler OD. Vascular pathology in Alzheimer disease: correlation of cerebral amyloid angiopathy and arteriosclerosis/Lipohyalinosis with cognitive decline. *J Neuropathol Exp Neurol* 2003;62:1287–1301.
- Pålhaugen L, Sudre CH, Tecelao S, et al. Brain amyloid and vascular risk are related to distinct white matter hyperintensity patterns. *J Cereb Blood Flow Metab* 2021;41:1162–1174.
- van Veluw SJ, Reijmer YD, van der Kouwe AJ, et al. Histopathology of diffusion imaging abnormalities in cerebral amyloid angiopathy. *Neurology* 2019;92(9):e933–e943.
- Haan J, Roos RAC, Algra PR, et al. Hereditary cerebral haemorrhage with amyloidosis-dutch type: magnetic RESONANCE imaging FINDINGS in 7 cases. *Brain* 1990;113:1251–1267.